

## JOURNAL NAME

# Synthesis of platinum group metal nanoparticles assisted by the electrochemical reduction of CO<sub>2</sub> at gas-diffusion electrodes

Omar Martinez-Mora,<sup>a,b</sup> Guillermo Pozo,<sup>a,c</sup> Luis Fernando Leon-Fernandez,<sup>a</sup> Jan Fransaer,<sup>b</sup> and Xochitl Dominguez-Benetton<sup>a,\*</sup>

- Separation and Conversion Technologies, VITO, Flemish Institute for Technological Research, Boeretang 200, 2400, Mol, Belgium.
- Department of Materials Engineering, Surface and Interface Engineered Materials, Katholieke Universiteit Leuven, Kasteelpark Arenberg 44 - box 2450, 3001 Leuven, Belgium.
- current address: Energy and Environment Division, TECNALIA, Mikeletegi Pasealekua 2, E-20009 Donostia-San Sebastián, Gipuzkoa, Spain.

\* Corresponding author: xoch@vito.be

## Electronic supplementary information (ESI)

### ESI-I Materials and Methods

#### Chemicals

Hexachloroplatinic (IV) acid (H<sub>2</sub>PtCl<sub>6</sub>, Pt 39.93 wt%) (Johnson Matthey), palladium (II) chloride (PdCl<sub>2</sub>, 99.9%) (Sigma-Aldrich), rhodium (III) chloride hydrate (RhCl<sub>3</sub>·xH<sub>2</sub>O, 99.98%) (Sigma-Aldrich), sodium chloride (NaCl, 99.5%) (Acros Organics), hydrochloric acid (HCl, 37 wt%) (Sigma-Aldrich), carbon dioxide (CO<sub>2</sub>, 99.998%) (Air Liquide), and argon (Ar, 99.99%) (Air Liquide) were purchased and used as received from different sources without any further purification. Demineralized water was used throughout the experiments to prepare aqueous solutions.

#### Electrochemical reactor

The electrochemical reactor (Fig S1) consisted of a three-compartment electrochemical cell. Through the first compartment, gas (i.e. CO<sub>2</sub>, Ar) flows at a fixed rate, with a set overpressure, at the hydrophobic layer of the gas diffusion electrode (GDE). The catholyte and anolyte flow from, and to, 3-necked bottles serving as reservoirs, through the respective cell compartment. Both, catholyte and anolyte compartment, are separated by a FUMASEPZ<sup>®</sup> FAP-4130-PK anion exchange membrane. Both liquid compartments have an exposed surface area of 10 cm<sup>2</sup> and a volume of 21 cm<sup>3</sup>. The GDE (VITO CORE<sup>®</sup>)<sup>1</sup> was composed of an outer active carbon-polytetrafluoroethylene (C-PTFE with a C to PTFE ratio of 80:20) layer pressed onto a stainless-steel mesh serving as current collector. The active carbon employed was Norit<sup>®</sup> SX 1G (Cabot, Europe). The projected surface area of such multilayered cathode was of 10 cm<sup>2</sup>, with a BET specific surface area of ~450 m<sup>2</sup> g<sup>-1</sup> for the PTFE-bound active layer. A Ag/AgCl (3M KCl) electrode was used as reference electrode, placed via Luggin capillary close to the GDE. A platinum-coated tantalum plate electrode (Pt 10 μm thicknes) was used as anode, this anode generated O<sub>2</sub> or Cl<sub>2</sub>, which had a negligible influence on the electrochemical (cathodic) process and products of interest.

#### Synthesis procedure.

0.1 M stock solutions of the three PGMs (H<sub>2</sub>PtCl<sub>6</sub>, PdCl<sub>2</sub>, RhCl<sub>3</sub>) were prepared in NaCl 0.5 M and used to further prepare the corresponding working solutions. The background electrolyte for the GDEx process consisted in a NaCl 0.5 M solution pH 3 adjusted with concentrated HCl. The catholyte solutions were prepared by mixing the background electrolyte and the PGMs stock solutions in order to have a final concentration of Pt<sup>4+</sup>, Pd<sup>2+</sup> and Rh<sup>3+</sup> of 3.0 mM, respectively. The background electrolyte alone (i.e., without PGMs) was used as anolyte. 250 mL or 100 mL of the catholyte and anolyte were collocated in the 3-necked glass bottles and connected to the electrochemical reactor using marprene tubing (Watson-Marlow) and pumped to their respective chamber with a flow rate of 40 mL min<sup>-1</sup> using a peristaltic pump (530, Watson-Marlow). The gases (i.e., CO<sub>2</sub>, Ar) were flown through the gas chamber at 200 mL min<sup>-1</sup>, with an overpressure of 20

mbar(g). The solutions and gases were flushed through the cell for 15 minutes before starting the experiments (without electrode polarization). Chronopotentiometric experiments were carried out in a batch mode at  $-10 \text{ mA cm}^{-2}$  using a Bio-Logic (VMP3) multichannel potentiostat. pH, charge, and potential were monitored throughout all experiments. The pH was measured every 5 seconds with a Metrohm 781 pH/ion meter equipped with a Metrohm Unitrode pH electrode. Aliquots of 1 ml were taken from the catholyte at different times, 100  $\mu\text{L}$  of HCl 0.1 M were added to quench the reaction and avoid precipitation of unreacted metal ions. The aliquots were centrifuged, and filtered with a 0.3  $\mu\text{m}$  pore filter. The filtered solutions were analyzed with an inductive coupled plasma-optical emission spectrometer (ICP-OES) (Varian 750 ES) to monitor the metal concentration in the liquid phase. The turning from a clear solution to a dark turbid solution was an indicative of the formation of the nanoparticles, together with appreciable light scattering using a red laser pointer against the electrolyte. The experiments were stopped when, after centrifuging an aliquot of the catholyte supernatant became transparent. The nanoparticles were left to settle down overnight. The supernatant was decanted, and the nanoparticles resuspended using demineralized water and centrifuged at 10000 rpm with a Hettich Rotina 35 centrifuge, to remove the remaining NaCl. The washing procedure was repeated until the conductivity of the supernatant was similar to the demineralized water. The products were dried under Ar atmosphere at room temperature and kept under storage for further characterization.

### Characterization

**X-ray diffraction (XRD):** The dried samples were analysed by powder X-ray diffraction in Seifert 3003 T/T diffractometer operated at a voltage of 40 kV and a current of 40 mA with Cu K $\alpha$  radiation ( $\lambda = 1.5406 \text{ \AA}$ ). The data were collected in the  $20^\circ$ - $120^\circ$  ( $2\theta$ ) range with a step size of  $0.05^\circ$ . The profile fitting of the powder diffraction patterns was performed with Highscore Plus (Malvern Pannalytical) using the inorganic crystal structure database (ICSD). Crystallite sizes were calculated using the Scherrer equation:<sup>2</sup>

$$D = (\kappa\lambda)/(\beta \cos\vartheta) \quad (1)$$

where  $D$  is the average crystallite size of the crystalline domains,  $\kappa$  is the Scherrer constant, typically considered 0.89 for spherical particles,  $\lambda$  is the X-ray wavelength,  $\beta$  is the line broadening at half the maximum intensity (FWHM) in radians, and  $\vartheta$  ( $^\circ$ ) is the Bragg angle at a reflecting plane.

**Electron Scanning Microscopy (SEM):** Micrographs of the dry samples were taken with a Philips XL30 FEG scanning electron microscope, Images presented were taken with secondary electrons and an acceleration voltage of 30 kV. The samples were prepared by dispersing the powders in ethanol and sonicating for 30 minutes. Then 10  $\mu\text{L}$  were dropped in a aluminum foil mounted on a sample holder. The mean particle size and distribution were evaluated by counting at least 100 particles using the software ImageJ (NIH). After that, data were fitted to a lognormal distribution to obtain the mean particle size and standard deviation.

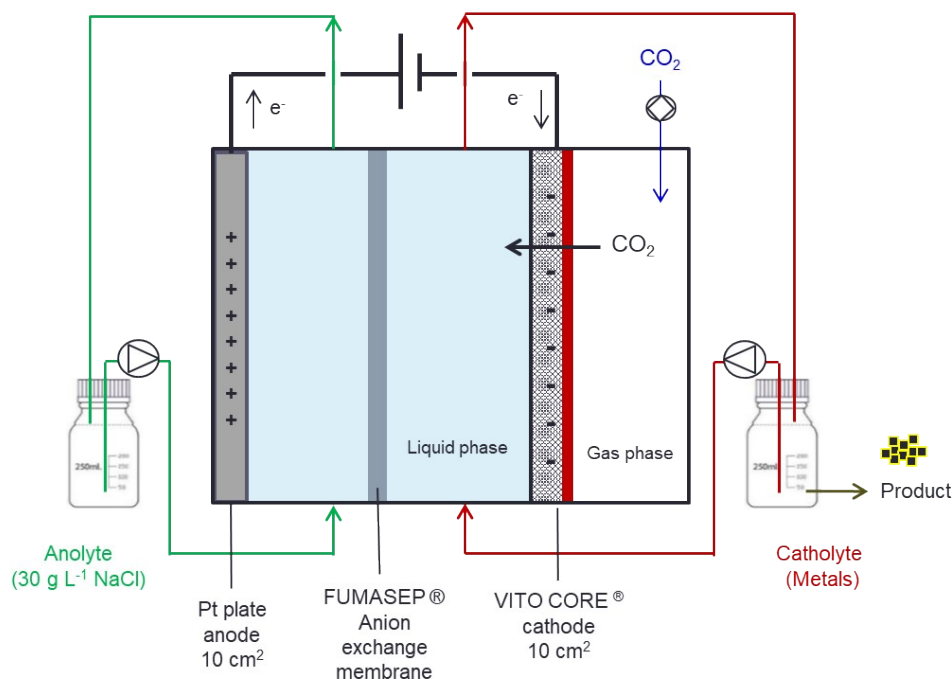
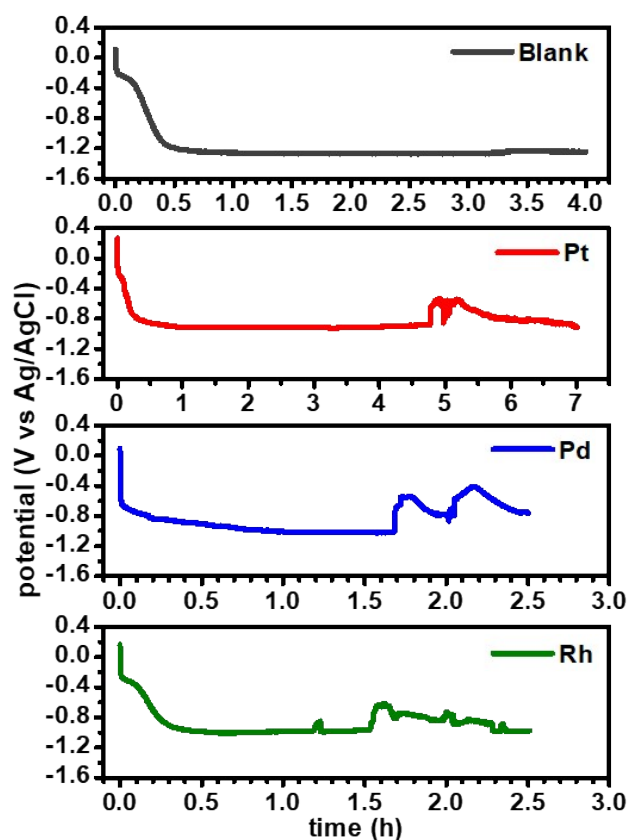


Fig S1. Schematic representation of the electrochemical reactor used for the GDEX experiments, exemplified with  $\text{CO}_2$  as the oxidizing gas to reduce at the gas-diffusion electrode.

ESI-II Supplementary data of the GDEx experiments with PGM ions precursors and CO<sub>2</sub>

**Fig. S2.** Photographs of the working solutions (250 mL each) at the beginning (left) and after the GDEx process (right) for a) Pt, b) Pd and c) Rh.



**Fig S3.** Chronopotentiometric curves for experiments performed at  $-10 \text{ mA cm}^{-2}$  using CO<sub>2</sub> as gas feedstock. The instability of the cathode potential observed is related to the presence of some the NPs formed in the catholyte that can block the luggin capillary interfering with the measured potential.

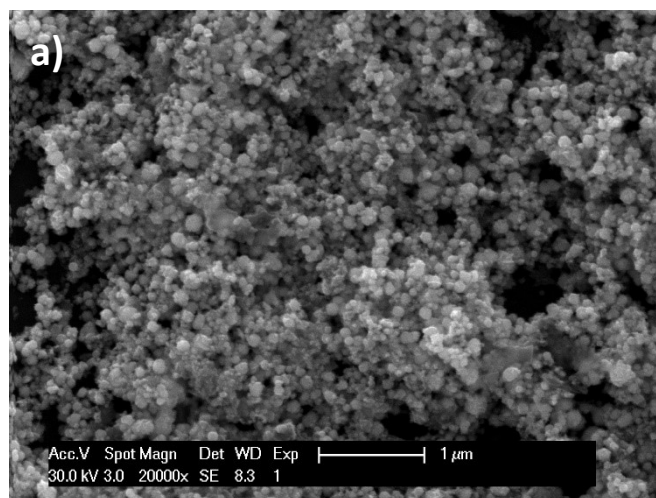
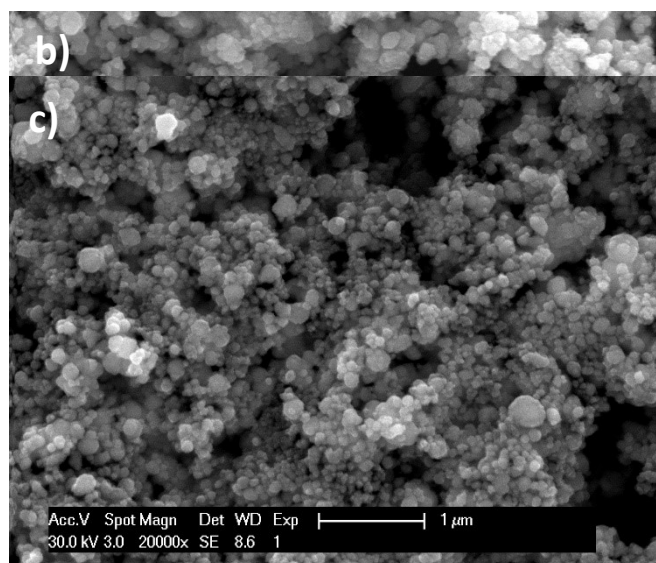


Fig S4. Full-size SEM images of the PGM nanoparticles synthesized using GDEx. a) Pt, b) Pd, c) Rh

#### ESI-III comparison of the different Pt NPs synthesized used H<sub>2</sub> and/or CO

In Table S1 the reports for the synthesis of Pt and Pd NPs using H<sub>2</sub> and/or CO as reducing agents are summarized, to the best of our knowledge there are no similar reports for Rh NPs.

**Table S1.** Comparison table of the different protocols to produce Pt NPs using H<sub>2</sub> and or CO reported in the literature and their size products



No.	Protocol	Size product	Conditions	Ref
1	H <sub>2</sub> was bubbled at high flow rate for 5 min to a solution containing 0.1 mM K <sub>2</sub> PtCl <sub>4</sub> and sodium polyacrylate (PANA) at different	4-18 nm	Room Temperature pH 7.5	3

	concentrations.			
2	H <sub>2</sub> was bubbled vigorously for 10 min to a solution containing 1 × 10 <sup>-3</sup> M – 1 × 10 <sup>-7</sup> M K <sub>2</sub> PtCl <sub>4</sub> and 0.1 M of PANa.	8-12 nm	Room Temperature	4
3	Pt NPs were preparing using solutions of K <sub>2</sub> PtCl <sub>4</sub> 0.1 mM – 0.5 mM containing citrate 6 × 10 <sup>-5</sup> M – 5 × 10 <sup>-4</sup> and flushing H <sub>2</sub> vigorously for 90 s and closed immediately afterwards. Depending on the composition of the solution the formation of NP lasted an hour or up to several days.	Less than 30 nm	Room Temperature pH 7 and 11	5
4	A solution of K <sub>2</sub> PtCl <sub>4</sub> 0.1 mM and poly(ethylene oxide)-poly(propylene oxide)-poly(ethylene oxide) (EO <sub>20</sub> PO <sub>70</sub> EO <sub>20</sub> ) copolymer (Pt-copolymer ratio 1:1) was bubbled with H <sub>2</sub> for five minutes, sealed and left under H <sub>2</sub> atmosphere overnight.	3-20 nm	Room temperature pH 7.5	6
5	Pt NPs were prepared using solution containing different concentrations of H <sub>2</sub> PtCl <sub>6</sub> (0.1 mM – 2 mM) and PVP (0.33g/mL) and flushing vigorously H <sub>2</sub> for 1 h.	0.8-14 nm	Room temperature	7
6	Electrogenerated Pt(II) and Pt(IV) soluble species were obtained using a Pt electrode by applying alternating potential for at least 1 hour, then they were reduced either by bubbling H <sub>2</sub> gas or electrogenerated H <sub>2</sub> at -2.0 to -0.1 V vs RHE.	5 to 38 nm	Room temperature 0.5 M H <sub>2</sub> SO <sub>4</sub> and 0.1 M HClO <sub>4</sub> were used as supporting electrolyte	8
7	Platinum acetylacetonate (Pt(acac) <sub>2</sub> ) was dissolved in acetone, impregnated onto a pre-treated silica support and dried under vacuum. The solid was subsequently heated to 200 °C for 1h in a gas mixture of CO and H <sub>2</sub> . A uniform dispersion of Pt nanocubes on the SiO <sub>2</sub> was obtained.	4-14 nm	200 °C	9
8	Carbon-supported Pt NPs were prepared dissolving Pt(acac) <sub>2</sub> in acetone and added to the carbon support. The mixture was dried and transferred to a tube furnace. The sample was reduced in a H <sub>2</sub> /CO mixture at 200 °C for 1 hour.	6-20 nm	200 °C	10
9	Pt NPs were made from Pt(acac) <sub>2</sub> in dodecylamine with a small amount of oleic acid using a hot injection GRAILS (gas reducing agent in liquid solution) approach. CO was used as the reducing and co-capping agent and yttrium acetylacetonate (Y(acac) <sub>3</sub> ) as additive.	8.8 ± 0.5 nm	210 °C	11
10	Pt nanocubes were prepared by dissolving Pt(acac) <sub>2</sub> in benzyl ether, oleylamine and oleic acid. CO was then introduced to the solution at room temperature and placed into a preheated oil bath. After 15 min of reaction at 200 °C the solution was allowed to cool down.	8.9 ± 0.5 nm	200 °C	12
11	Pd NPs were prepared in a water-in-CO <sub>2</sub> microemulsion by H <sub>2</sub> reduction of Pd <sup>2+</sup> . PdCl <sub>2</sub> (0.04 M) was mixed with sodium bis(2-ethylhexyl)sulfosuccinate [AOT] (15 mM) and perfluoropolyether phosphate [PFPE-PO <sub>4</sub> ] (30 mM).	5-10 nm	Room temperature 80 atm CO <sub>2</sub> 10 atm H <sub>2</sub>	13
12	Pd NPs in a water/AOT/n-hexane microemulsion by H <sub>2</sub> gas reduction of PdCl <sub>4</sub> <sup>2-</sup>	4-10 nm	Room temperature 1 atm H <sub>2</sub>	14
13	Pd NPs were prepared using an aqueous solution of tetraaminepalladium(II) chloride [Pd(NH <sub>3</sub> ) <sub>4</sub> ]Cl <sub>2</sub> with Pd(II) concentration of 0.1-0.75 mM and a ratio of 1 : 10 and 1 : 20 for PANa and sodium polyphosphate (PPNa) and saturating with H <sub>2</sub>	30-50 nm	Room temperature	15
14	Pd NPs were prepared using PdCl <sub>2</sub> and PVP as a surfactant. H <sub>2</sub> (50 ml/min) was used as reducing agent.	136-271 nm	Room temperature	16
15	Pd NPs were prepared by mixing 160 mg PVP and 25 mg Pd(acac) <sub>2</sub> in 10 mL DMF. CO, H <sub>2</sub> and CO/H <sub>2</sub> were bubbled continuously into the solution at a flow rate of 0.033 mL s <sup>-1</sup> . The solution was heated at 100 °C for 3 h under atmospheric pressure.	55 ± 2 nm (CO) 35 ± 2 nm (CO/H <sub>2</sub> ) ~68 ± 11* (H <sub>2</sub> )	100 °C	17
16	See ESI-I materials and methods	109 ± 45 nm (Pt)	Room temperature No additives	This work

		151 ± 49 nm (Pd)	No supporters	
		156 ± 57 nm (Rh)		

\* Calculated from the TEM image presented in the article.

#### ESI-IV Experiments for the selectively recovery of PGMs using GDEx

To demonstrate the possibility to use the GDEx process for the selectively removal of PGMs solutions containing  $\text{Rh}^{3+}$  at concentrations of 1.0 to 6.0 mM containing additionally other metals in solutions at higher concentrations ( $\text{Al}^{3+}$  185 mM,  $\text{Mg}^{2+}$  41 mM and  $\text{Fe}^{2+}$  18 mM) the solutions were prepared using HCl 1M as matrix. The pH of the was around 0.25. 250 mL of these solutions were used as catholyte and 250 mL of NaCl 0.5 M as anolyte. The GDE was polarized at -1.4 V vs Ag/AgCl and the experiment was run until the solution reached a pH of 2. The solid was washed according to the cleaning procedure and characterized metallic Rh using XRD (Fig S4). The concentration of the metals was measured at the beginning and at the end of the experiments and the % of removal is reported in the table S2. As it can be seen while Rh has been completely removed, the other metals were kept in solution, showing that GDEx process can be used to selectively recover PGMs from aqueous solutions containing metals at higher concentrations if the pH conditions are kept acidic as  $\text{H}_2$  will reduce only the PGMs at room temperature but no other metals.

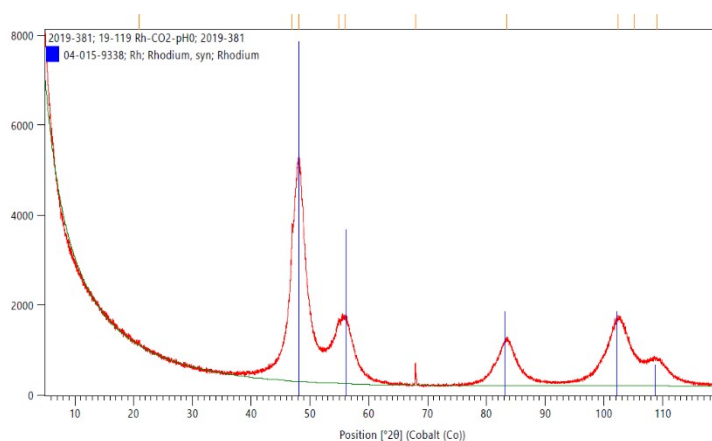


Fig. S5. X-ray diffraction pattern of the product obtained for the Rh solution.

Table S2. % of metal removal of the Rh, Al, Mg and Fe the experiments

Initial Rh concentration	% of metal removal			
	Mg	Al	Fe	Rh
6.0 mM	4,8	4,1	7,6	99,5
3.5 mM	9,9	8,8	11,0	99,3
1.0 mM	17,4	15,8	5,3	98,1

#### ESI-V Experiments replacing the $\text{CO}_2$ by Ar at the gas compartment.

To demonstrate the role of the  $\text{CO}_2$  equilibrium to buffer the pH during the GDEx process,  $\text{CO}_2$  was replaced by Ar and the cathode was polarized at the same current density. As expected, when only the water reduction reaction takes place, due to the generation of  $\text{OH}^-$  ions, the pH increases from 3 to 11.5 without any noticeable buffered zone. The same experiment was repeated with solutions containing the metals. For the case of Pd and Rh, the  $\text{OH}^-$  displaces the  $\text{Cl}^-$  of the  $[\text{PdCl}_4]^{2-}$  and  $[\text{RhCl}_6]^{3-}$  to form hydroxide complexes.  $\text{Rh}(\text{OH})_3$  precipitate as such, while  $\text{Pd}(\text{OH})_2$  is highly unstable and is easily transformed into hydrated  $\text{PdO}$ ,<sup>18</sup> as is shown in the X-ray diffraction patterns (Fig. S5b and Fig. S5c). The consumption of  $\text{OH}^-$  is noted in the pH plateau in the experiments with Pd and Rh, before reaching pH 11. For the case of Pd, in the X-ray diffraction patterns (Fig. S5b) peaks corresponding to the metallic

Pd were identified suggesting that a small amount to  $\text{Pd}^{2+}$  was reduced to  $\text{Pd}^0$ . These results highlight the importance of the  $\text{CO}_2$  equilibrium in the GDE process.

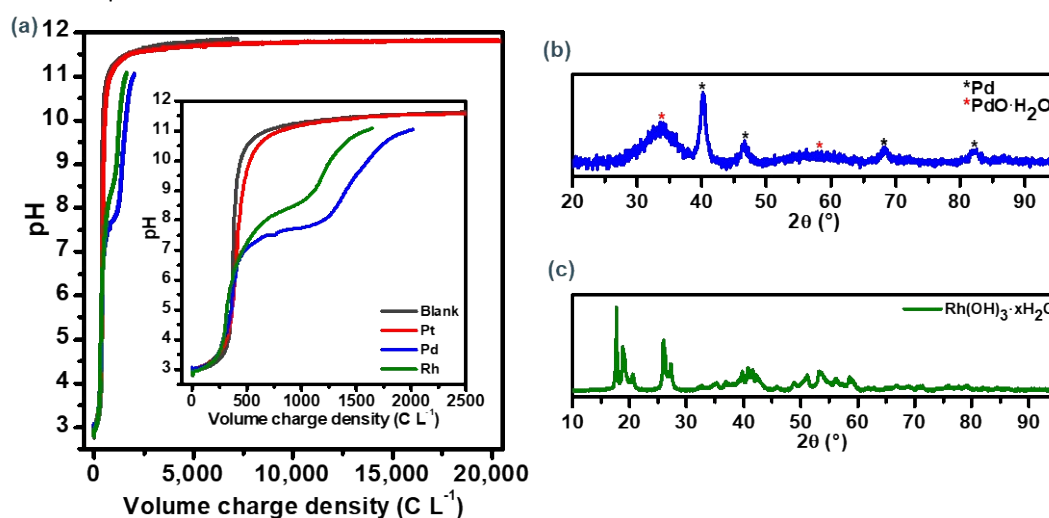


**Fig S6.** **a)** Evolution of pH as function of charge consumed throughout the GDE process when  $\text{CO}_2$  is replaced with Ar. **b)** X-ray diffraction pattern of the product obtained for the Pd solution. **c)** X-ray diffraction pattern of the product obtained for the Rh solution.

#### ESI-VI Experiments flowing Ar at the gas phase of the GDE reactor and bubbling $\text{CO}_2$ in the catholyte reservoir.

To demonstrate the role of the CO generated during the  $\text{CO}_2$  reduction at the GDE during the GDE process, Ar was flowed in the gas compartment of the reactor and  $\text{CO}_2$  was bubbled in the catholyte reservoir. The cathode was polarized at the same current density. At these conditions water reduction to  $\text{H}_2$  and  $\text{CO}_2$  equilibrium at the bulk electrolyte take place but not the  $\text{CO}_2$  reduction to CO. As expected, the pH of the catholyte is buffered (in both, blank and containing metals experiments) at  $\sim 6$ . As in the GDE process (in which  $\text{CO}_2$  is reduced at the GDE) metallic nanoparticles were obtained. However the average diameter of these products was bigger and with a broader distribution.

These results highlight the importance of the formation and presence of CO in the GDEx process to control the size and distribution of the products obtained.

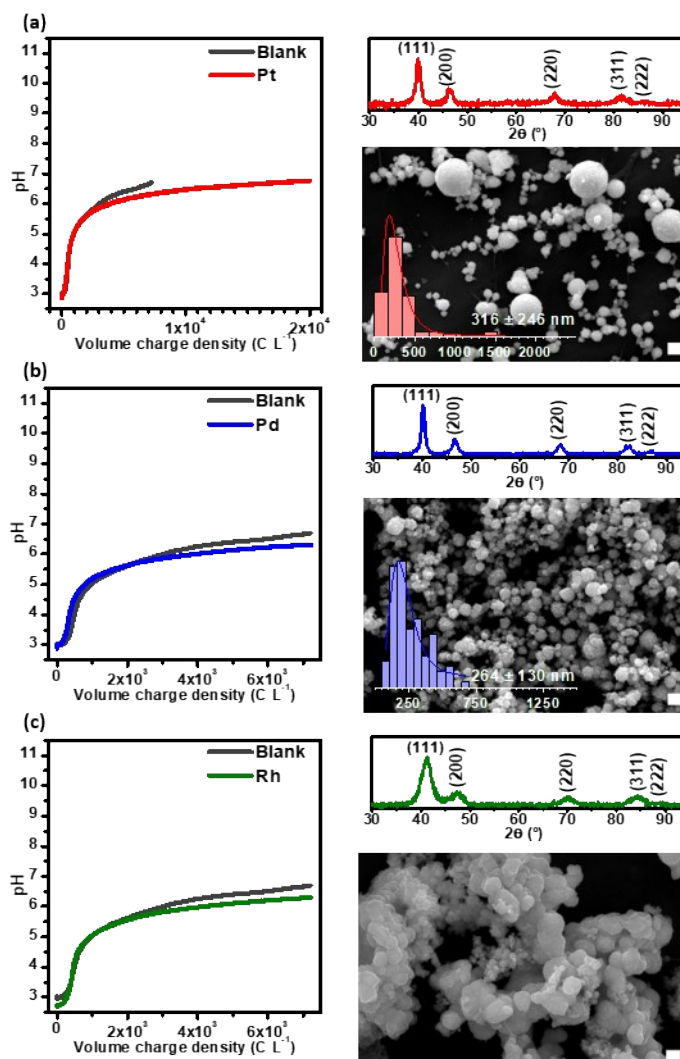


**Fig. S7.** Left: Evolution of pH a function of the charge consumed per unit volume throughout the GDEx process when Ar is flowed at the gas phase and CO<sub>2</sub> is bubbled at the catholyte reservoir yielding elemental nanoparticles. Right: X-Ray diffraction patterns (up) and SEM micrographs and distribution histograms (down) of the elemental nanoparticles. The white scale bar is 500 nm. (a) Pt\*; (b) Pd; (c) Rh.

## ESI References

- 1 Y. Alvarez-Gallego, X. Dominguez-Benetton, D. Pant, L. Diels, K. Vanbroekhoven, I. Genné and P. Vermeiren, *Electrochim. Acta*, 2012, **82**, 415–426.

- 2 C. F. Holder and R. E. Schaak, *ACS Nano*, 2019, **13**, 7359–7365.
- 3 T. S. Ahmadi, Z. L. Wang, T. C. Green, A. Henglein and M. A. El-Sayed, *Science (80-. )*, 1996, **272**, 1924 LP – 1925.
- 4 G. S. Devi and V. J. Rao, *Bull. Mater. Sci.*, 2000, **23**, 467–470.
- 5 A. Henglein and M. Giersig, *J. Phys. Chem. B*, 2000, **104**, 6767–6772.
- 6 Z. Kónya, V. F. Puentes, I. Kiricsi, J. Zhu, P. Alivisatos and G. A. Somorjai, *Catal. Letters*, 2002, **81**, 137–140.
- 7 Z. Tang, D. Geng and G. Lu, *J. Colloid Interface Sci.*, 2005, **287**, 159–166.
- 8 C. F. Zinola, *J. Electrochem. Soc.*, 2017, **164**, H170–H182.
- 9 Z. Peng, C. Kisielowski and A. T. Bell, *Chem. Commun.*, 2012, **48**, 1854–1856.
- 10 C. Zhang, S. Y. Hwang and Z. Peng, *J. Mater. Chem. A*, 2013, **1**, 14402–14408.
- 11 W. Zhou, J. Wu and H. Yang, *Nano Lett.*, 2013, **13**, 2870–2874.
- 12 Y. Kang, X. Ye and C. B. Murray, *Angew. Chemie Int. Ed.*, 2010, **49**, 6156–6159.
- 13 H. Ohde, C. M. Wai, H. Kim, J. Kim and M. Ohde, *J. Am. Chem. Soc.*, 2002, **124**, 4540–4541.
- 14 B. Yoon, H. Kim and C. M. Wai, *Chem. Commun.*, 2003, 1040–1041.
- 15 R. D. Solovov and B. G. Ershov, *Colloid J.*, 2014, **76**, 595–599.
- 16 S. C. Kim, S. C. Jung, Y.-K. Park, H. G. Ahn and S. G. Seo, *J. Nanosci. Nanotechnol.*, 13, 1961–1965.
- 17 H. Zhu, Q. Chi, Y. Zhao, C. Li, H. Tang, J. Li, T. Huang and H. Liu, *Mater. Res. Bull.*, 2012, **47**, 3637–3643.
- 18 J. Ma, Y. Ji, H. Sun, Y. Chen, Y. Tang, T. Lu and J. Zheng, *Appl. Surf. Sci.*, 2011, **257**, 10483–10488.